

BL28B2

White Beam X-ray Diffraction

1. Introduction

BL28B2 is dedicated to multiple techniques using white X-rays in several research fields. It is a bending magnet beamline that provides white X-rays from a bending magnet source without passing through any optical devices. The techniques involve X-ray diffraction, X-ray microtomography (micro-CT), and ultrafast X-ray radiography. Thus, the beamline supports various experiments such as the evaluation of structure materials using white X-ray diffraction and the three-dimensional observation of metallic objects and highly dense materials such as fossils and concrete using high-energy X-ray micro-CT. To improve and upgrade the measurement techniques using this beamline, the research and development of experimental techniques and instruments was conducted in FY2022.

2. Upgrades of measurement techniques

2-1. X-ray Diffraction

BL28B2 can be used for energy-dispersive X-ray diffraction experiments, which are capable of obtaining diffraction profiles from selected regions within a sample in a relatively short measurement time. The obtained diffraction profiles are used to evaluate the distortion of metal materials and to identify minerals in concretes, for example.

In the identification of minerals, the intensity ratio of the diffraction peaks in the profiles is important information. Therefore, we have prepared dedicated software to calculate the energy-dispersive X-ray diffraction profiles. Figure 1 shows a graphical user interface (GUI) of the software. The chart at the top of the figure is the

calculated diffraction profiles of CeO_2 . The calculation formula is as follows:

$$I = \lambda^3 |F(hkl)|^2 P \left(\frac{1 + \cos^2 2\theta}{\sin^2 \theta \cos \theta} \right). \quad (1)$$

Here, I is the diffraction intensity, F is a structure factor of reflection hkl , P is a multiplicity factor, and θ is the Bragg angle. The chart shown by the red line in the bottom figure is the measured diffraction profile. The peaks near 34 keV and 40 keV are due to fluorescent X-rays from Ce. In comparison, the chart shown by the blue line is a calculated diffraction profile multiplied by the spectrum of the incident X-rays and the X-ray transmission of the sample. It can be seen that the calculated result is generally consistent with the measured one.

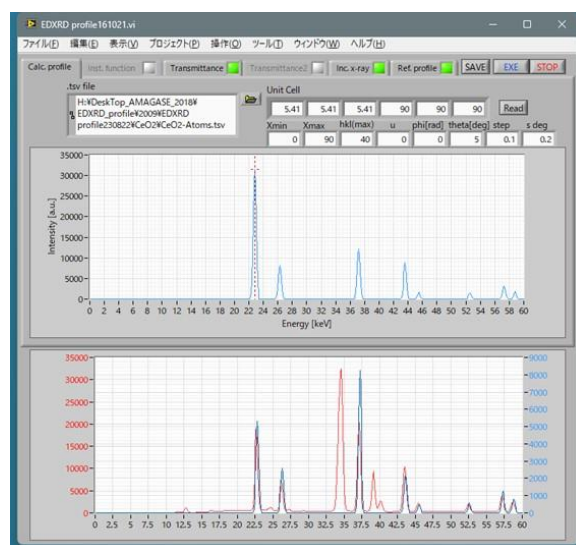


Fig. 1. Main panel of our calculation software of energy-dispersive diffraction profiles.

A list of the diffraction indices of the diffraction peaks is displayed in a separate window, as shown in Fig. 2. In the chart at the top of Fig. 1, the diffraction index of the diffraction peak pointed

to by the cursor is indicated in the list. The calculated results can be saved as a text file, as shown in Fig. 3. The calculated values of the diffraction profile, the incident X-ray spectrum, and the X-ray transmission of the sample are listed in separate columns.

[keV]	h	k	l
22.757	1	1	1
26.277	0	0	2
37.161	0	2	2
43.576	1	1	3
45.513	2	2	2
52.554	0	0	4
57.270	1	3	3
58.757	0	2	4
64.366	2	2	4
68.270	1	1	5
68.270	3	3	3
74.323	0	4	4
77.729	1	3	5
78.831	0	0	6
78.831	2	4	4
83.096	0	2	6

Fig. 2. A panel of the table showing diffraction indices.

Energy [keV]	[Calc. profile]	[Inc. X-ray]	[Absorption]	[Ref. profile]	Background
0.00000	0.00000	1.00000	0.00000	0.00000	0.00000
0.10000	0.00000	0.00000	0.00000	0.00000	0.00000
0.20000	0.00000	0.00000	0.00000	0.00000	0.00000
0.30000	0.00000	0.00000	0.00000	0.00000	0.00000
0.40000	0.00000	0.00000	0.00000	0.00000	0.00000
0.50000	0.00000	0.00000	0.00000	0.00000	0.00000
0.60000	0.00000	0.00000	0.00000	0.00000	0.00000
0.70000	0.00000	0.00000	0.00000	0.00000	0.00000
0.80000	0.00000	0.00000	0.00000	0.00000	0.00000
0.90000	0.00000	0.00000	0.00000	0.00000	0.00000
1.00000	0.00000	0.00000	0.00000	0.00000	0.00000
1.10000	0.00000	0.00000	0.00000	0.00000	0.00000
1.20000	0.00000	0.00000	0.00000	0.00000	0.00000
1.30000	0.00000	0.00000	0.00000	0.00000	0.00000
1.40000	0.00000	0.00000	0.00000	0.00000	0.00000
1.50000	0.00000	0.00000	0.00000	0.00000	0.00000
1.60000	0.00000	0.00000	0.00000	0.00000	0.00000
1.70000	0.00000	0.00000	0.00000	0.00000	0.00000
1.80000	0.00000	0.00000	0.00000	0.00000	0.00000
1.90000	0.00000	0.00000	0.00000	0.00000	0.00000
2.00000	0.00000	0.00000	0.00000	0.00000	0.00000
2.10000	0.00000	0.00000	0.00000	0.00000	0.00000
2.20000	0.00000	0.00000	0.00000	0.00000	0.00000
2.30000	0.00000	0.00000	0.00000	0.00000	0.00000
2.40000	0.00000	0.00000	0.00000	0.00000	0.00000
2.50000	0.00000	0.00000	0.00000	0.00000	0.00000
2.60000	0.00000	0.00000	0.00000	0.00000	0.00000
2.70000	0.00000	0.00000	0.00000	0.00000	0.00000
2.80000	0.00000	0.00000	0.00000	0.00000	0.00000
2.90000	0.00000	0.00000	0.00000	0.00000	0.00000
3.00000	0.00000	0.00000	0.00000	0.00000	0.00000

Fig. 3. An example of calculation results of the diffraction profile.

2-2. Introduction of automatic X-ray micro-CT system

Since BL28B2 is capable of providing white X-rays from the bending magnet source, it is possible to use the high-energy white X-rays, which have a peak energy of around 200 keV, by suppressing the lower energy X-rays using a heavy-metal filter [1]. The high penetration power of the X-rays with 200 keV

allows us to observe the inner structures of metal objects and dense materials such as fossils and concrete by means of X-ray micro-CT [2]. In addition, the relatively high spatial coherence of the X-rays makes it possible to conduct X-ray phase-contrast imaging based on the large propagation distance even in the high-energy region. This property provides an opportunity to observe both soft materials composed of light elements and metallic structures simultaneously. Therefore, X-ray micro-CT at the 200 keV region is a highly versatile tool and can be expected to be applied to various samples. Below, an automatic X-ray micro-CT (ACT) system based on the high-energy X-ray micro-CT developed so far is introduced.

A schematic drawing of the ACT system is shown in Fig. 4. The sample exchange, which was previously performed manually, can be done automatically by a sample exchange robot. Sample stockers are provided on both sides of the robot, and the specified sample can be automatically set on the sample stage. A photograph of the sample exchange robot and sample stockers is shown in Fig. 5. To avoid radiation damage to the robot and its controlling board owing to scattered high-energy X-rays, they are housed in a protective cage composed of lead and stainless-steel plates. The sample placed on the sample stage can be automatically measured under prespecified measurement conditions. After the measurement, data transfer to a high-performance computing system and processing for reconstructing images can be done almost completely automatically. For the tomographic measurement, a dedicated sample holder was developed to simplify the alignment of the sample position and clarify the sample size and the measurement range along the vertical direction of

the sample.

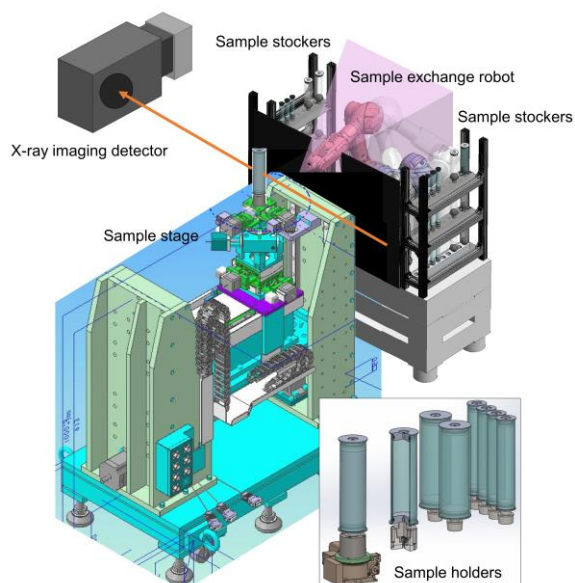


Fig. 4. Schematic drawing of an automatic X-ray micro-CT system.

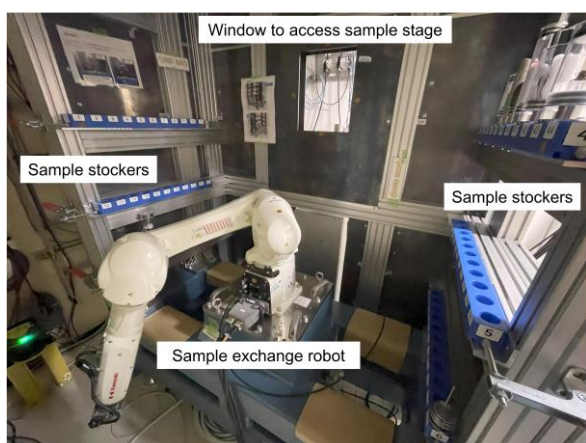


Fig. 5. Photograph of a sample exchange robot and sample stockers (inside of a protective housing).

The maximum field of view in the ACT system depends on the beam size at the X-ray energy of 200 keV, which is 48 mm in width and 1.2 mm in height. By scanning the sample in the vertical direction and repeating the measurement, it is possible to extend the vertical field of view. It takes approximately 1.5 hours to measure the sample of

48 mm width and 10 mm height, depending on the measurement conditions. The effective pixel size of the specially developed visible-light-conversion-type X-ray imaging detector is $3.44\ \mu\text{m}$, while measurements with 2×2 binning (pixel size: $6.88\ \mu\text{m}$) or 3×3 binning (pixel size: $10.32\ \mu\text{m}$) are also possible in accordance with the required spatial resolution. Since the X-ray imaging detector employs an ultrahigh-definition CMOS camera, it can cover the field of view of more than 46 mm in width with the pixel size of $3.44\ \mu\text{m}$. In this case, the reconstructed image is composed of over $13,600 \times 13,600$ pixels. The reconstructed images can be downloaded from a dedicated website. As an example of the measurement with the ACT system, a longitudinal sectional image of an 18650 standard battery measured with the pixel size of $3.44\ \mu\text{m}$ is shown in Fig. 6.

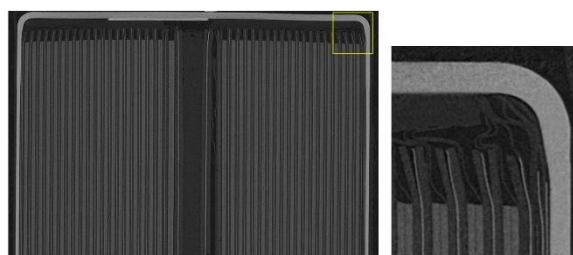


Fig. 6. Longitudinal sectional image of an 18650 standard battery (left). Magnified image at the square region (right).

A remarkable feature of the ACT system is its convenience of simply sending the sample in the dedicated sample holder and downloading the resultant images after a short time. This system is expected to be utilized in various fields because it can easily acquire ultrahigh-definition 3D images of relatively large samples such as electronic devices and rocks.

Hoshino Masato, Kajiwara Kentaro, Uesugi
Kentaro, and Yasutake Masahiro
Japan Synchrotron Radiation Research Institute

References:

- [1] Hoshino, M. Uesugi, K. Shikaku, R. & Yagi, N.
(2017). *AIP Adv.* **7**, 105122.
- [2] Hoshino, M. Uesugi, K. & Yagi, N. (2020). *J.*
Synchrotron Rad. **27**, 934-940.